Journal of Alloys and Compounds 509 (2011) 1505–1510

Contents lists available at ScienceDirect

Journal of Alloys and Compounds

journal homepage: www.elsevier.com/locate/jallcom

A systematic study on the synthesis of Ca, Gd codoped cerium oxide by combustion method

A. Ainirad [a], M.M. Kashani Motlagh [a,*], A. Maghsoudipoor [b]

[a] Department of Chemistry, University of Science and Technology of Iran, Tehran, Iran
[b] Department of Ceramics, Materials and Energy Research Center, Karaj, Iran

ARTICLE INFO

Article history:
Received 24 June 2010
Received in revised form 17 October 2010
Accepted 27 October 2010
Available online 3 November 2010

Keywords:
Ceramics
Ionic conduction
Combustion synthesis
Doped ceria

ABSTRACT

Co-doped of CeO_2 nanopowders are ideal electrolyte materials for intermediate temperature solid oxide fuel cells. In this work, $Ce_{1-(x+y)}Gd_xCa_yO_{2-(0.5x+y)}$ nanopowders are successfully synthesized by a glycine–nitrate combustion process. Then calcination was carried out at 450, 700, 850, 950 and we found that calcined powders were single phase by room temperature X-ray diffraction (XRD) and have an average crystallite size of 45 nm (based on Scherrer formula). Scanning electron microscopy (SEM) was employed to characterize the morphology of powder. Finally we studied the effect of fuel to nitrate ratio on the properties of resulting powders.

1. Introduction

Solid oxide fuel cell (SOFC) has attracted much attention in recent years because of its high-energy conversion efficiency and environmental friendship. In fact, solid oxide fuel cells (SOFCs) are electrochemical devices that convert the chemical energy of a fuel into electrical energy in a clean, cheap and efficient way and Consist of three parts, including anode, cathode and electrolyte [1].

Conventional SOFCs which use yttria-stabilized zirconia (YSZ) as an electrolyte are operated at around 1273 K. However, such high temperatures often lead to some problems such as solid-state reactions between the components, thermal degradation and thermal expansion mismatch. Thus, reducing the operating temperature of the SOFCs becomes increasingly important. One of the most promising methods for realizing intermediate temperature solid oxide fuel cells (ITSOFCs) operating below 1073 K is to replace YSZ with other electrolytes with higher oxygen ionic conductivity at low temperature [1].

Doped ceria is a potential electrolyte material for ITSOFCs because it shows much higher oxygen ionic conductivity than YSZ [2,3]. Ceria itself is not a good ionic conductor, but ionic conductivity increases significantly with the introduction of oxygen vacancies caused by the doping of ceria with two or more components at the same time and the research results showed that complex doping with several rare earth or/and alkali earth elements was an effective method to improve the ionic conductivity of the electrolyte [4–7].

Hurley and Hohnke [8] studied the electrical properties of solid state synthesized $Ce_{1-x}Ca_xO_{2-\delta}$ samples that were sintered at 1650 °C for 4 h. Yahiro et al. [9] reported the correlation of electrical properties and microstructures of solid state synthesized ceria alkaline earth oxide systems. Huang et al. [10] reported the hydrothermal synthesis and properties of $Ce_{1-x}Ca_xO_{2-\delta}$ solid solutions, where a sintering temperature of 1400 °C was reported for achieving 95% sintered density. Recently, Peng et al. [11] reported the synthesis of nanocrystalline $Ce_{1-x}Ca_xO_{2-\delta}$ solid solutions by nitrate citrate combustion synthesis. Rodriguez et al. [12] investigated the structural and electronic properties of $Ce_{1-x}Ca_xO_{2-\delta}$ systems. Yamashita et al. [13] and Sato et al. [14] explored the UV shielding characteristics of calcia-doped ceria systems and observed an increased UV shielding property of calcia-doped ceria systems. The results indicated that co-doping method was proved to be effective to improve the electrical property of the ceria-based electrolytes.

In the past few years, combustion synthesis of multi component ceramic oxides has been gaining reputation as a straightforward preparation process to produce homogeneous, very fine, crystalline and unagglomerated powders [15,16]. The basis of the combustion synthesis technique comes from the thermo chemical concepts used in the field of propellants and explosives [17].

In the present work, we used the glycine–nitrate solution combustion synthesis technique to obtain nanocrystalline $Ce_{1-(x+y)}Gd_xCa_yO_{2-(0.5x+y)}$ powder. Synthesized powder was then calcined to remove any traces of organic compounds. The calcined

* Corresponding author. Tel.: +98 21 77240288; fax: +98 91 26766553.
E-mail address: m.kashani@iust.ac.ir (M.M. Kashani Motlagh).

0925-8388/$ – see front matter © 2010 Elsevier B.V. All rights reserved.
doi:10.1016/j.jallcom.2010.10.137

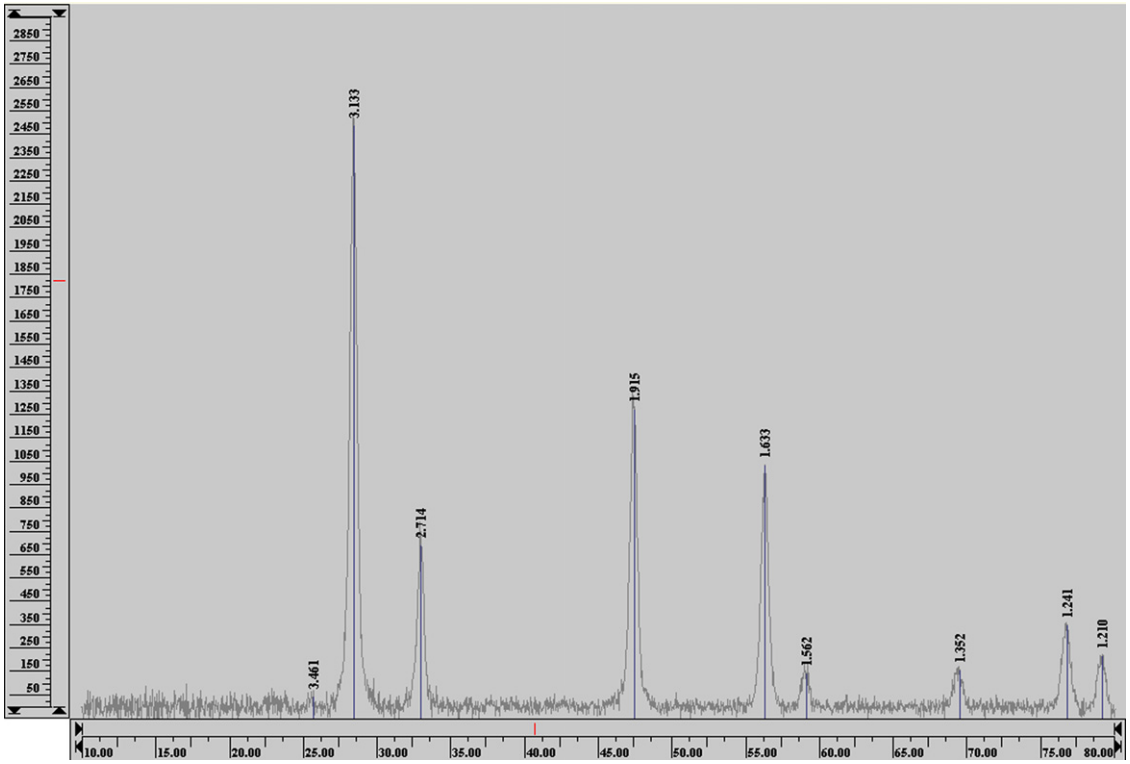

Fig. 1. XRD pattern of the calcined $Ce_{1-(x+y)}Gd_xCa_yO_{2-(0.5x+y)}$ powder.

powder was pelletized with hydraulic press machine in circular disk shaped pellet and it was also sintered to obtain to a dense pellet for using as the electrolyte in SOFCs.

We also investigated the role of fuel-to-oxidant ratio, dopant concentration on combustion process and properties of the resulted nanopowders.

2. Experimental

According to the results of researches, sintering of obtained pellets at high temperature (>1300 °C) results into reduction of CeO_2 to Ce_2O_3 (valency changes from $Ce^{4+} \rightarrow Ce^{3+}$), this reduction leads to a decrease in oxygen vacancies and density of the sintered pellets. It was expected that this reduction and the corresponding oxygen evolution could be suppressed by doping ceria with lower valent metal ions having larger cationic size than Ce^{4+} such as Ca^{2+} [18]. Doped ceria with 10 mol% of Gd was shown to have the highest of the ionic conductivity [19,20].

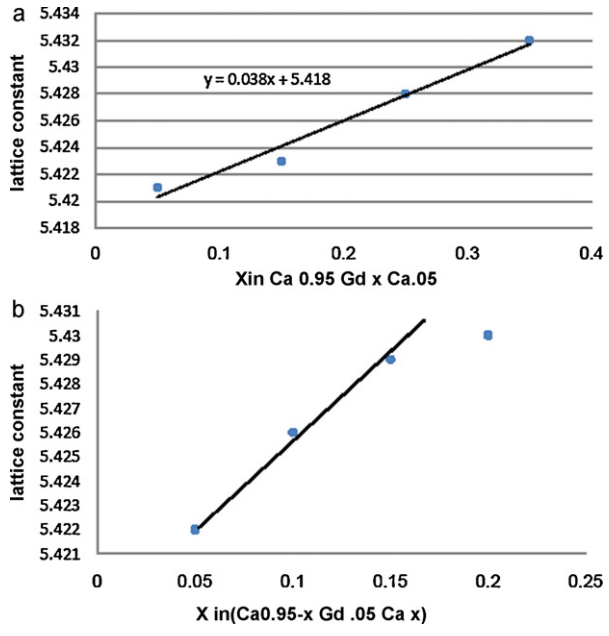

Fig. 2. Lattice constant for doped ceria as a function of dopant concentration.

Thus we synthesized a series of codoped ceria with different Gd and Ca content. We also used two types of fuels (glycine and urea) to investigate the effects of reactivity and rate of reaction between the fuel and metal nitrates on the morphology of the resulted powders.

The required molar ratio of metal nitrates and glycine was calculated based on the propellant chemistry, i.e. the ratio of oxidizing and reducing valencies should be unity. The oxidizing valencies of cerium nitrate and gadolinium nitrate are −15 and that of calcium nitrate is −10, the reducing valencies of glycine and urea are +9 and +6 respectively [21,22]. Therefore based on the propellant chemistry, reaching to 1 mol of $Ce_{1-(x+y)}Gd_xCa_yO_{2-(0.5x+y)}$, in order to release the maximum energy, needs $(15-5y)$/9 mol of glycine or $(15-5y)$/6 mol of urea. The formation of solid solution may be presented by the following reaction:

$$1-(x+y)Ce(NO_3)_3{\cdot}6H_2O + xGd(NO_3)_3{\cdot}6H_2O + yCa(NO_3)_3{\cdot}6H_2O + mC_2H_5NO_2$$
$$\rightarrow Ce_{1-(x+y)}Gd_xCa_yO_{2-(0.5x+y)} + (5/2)mH_2O(g)$$
$$+ (3-y+m)/2N_2(g) + 2mCO_2(g)$$

At first, the metal nitrates and glycine were dissolved in double distilled water and then pH value of solution was adjusted at 8 by adding ammonium hydroxide. In the next step, the obtained translucent solution was heated at 80 °C to remove the excessive water until it turned into a viscose gel.

The heating was continued up to 300 °C to cause the auto-ignition. The auto-ignition released a large volume of gases and the voluminous powder was produced. During the ignition, the container was covered with a fine-mesh sieve to prevent the powder from flying out of its container. Then calcination of the powder was carried out at four different temperatures (450, 700, 850 and 950 °C) for 3 h to remove any traces of fuel and to obtain pure phase of the powder.

The crystalline phases were identified by X-ray diffraction analysis (XRD)-using an X-ray diffractometer (Siemens D5000) and Cu Kβ radiation (λ = 0.15418 nm). The average crystallite size, D, was estimated by using the Scherrer formula: $D = (0.9\lambda)/(\beta \cos\theta)$ [23] in which, β is the line broadening measured at half of height of peak, θ is the angle of reflection and λ is the wavelength of radiation.

The lattice parameters were calculated by using formula which is shown below [24]:

$$\frac{1}{d_{hkl}^2} = \frac{h^2}{a^2} + \frac{k^2}{b^2} + \frac{l^2}{c^2}$$

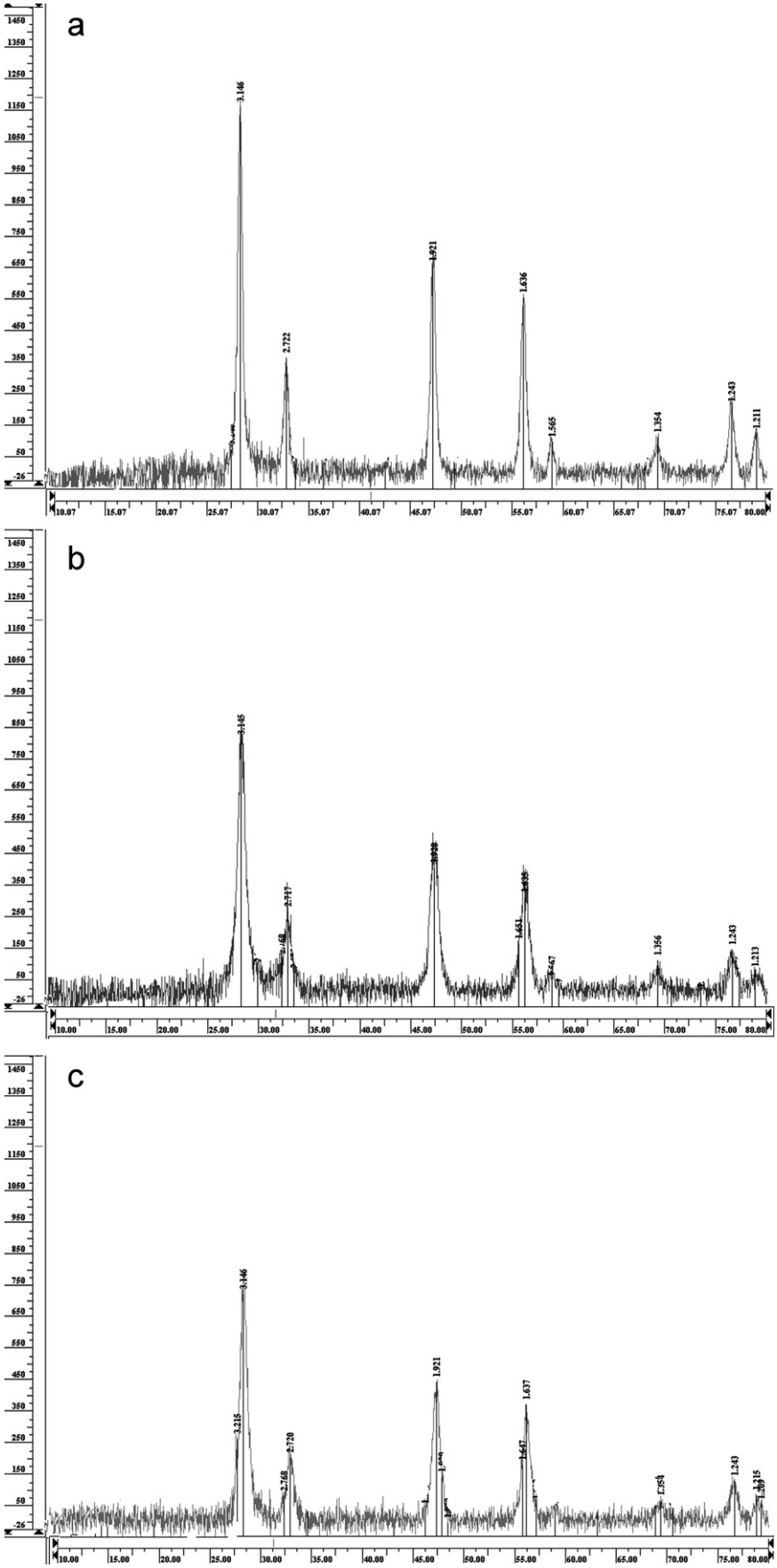

Fig. 3. XRD patterns of synthesized powder's samples trough combustion of different fuel to oxidant ratios. (a) O/F = 1.33, (b) O/F = 1.66, (c) O/F = 1.96.

In which, d is the interplanar distance, (h, k, l) are the miller indices for the corresponding d-spacing and a, b, c are the lattice parameters. Scanning electron microscopy (SEM) was used to morphological studies.

3. Results

3.1. X-ray diffraction (XRD) studies

3.1.1. Phase structure

Fig. 1 shows the XRD pattern of the calcined powder at 850 °C indicating the presence of a single phase with cubic fluorite structure. No peaks of un-reacted CaO and Gd_2O_3 are observed, this issue suggests in-situ solid solution formation. The calculated lattice parameter is 5.41 Å, which is in well agreement with the reported values. The calculated crystallite size by Scherrer method is 45 nm. It was also found that the calcination of synthesized powder at 850 °C is not showing a significant change in the crystallite size. The formation of nanocrystalline structure indicated by XRD was further supported by SEM studies.

3.1.2. Dopant concentration

The changes of the lattice parameter of doped ceria as a function of dopant concentration are shown in Fig. 2. It can be seen that the lattice parameters are increased with increasing dopant content for each of dopants. But it should be noted that, the slope of the changes for Ca is larger than Gd. This is because of the ionic radius of Ca^{2+} (0.126 nm) which is larger than ionic radius of Gd^{3+} (0.1053 nm), and both of them are larger than the critical radius of Ce^{4+} (0.1019 nm) [25,26].

The figure clearly reveals that, the changes of lattice parameter are not increased linearly in 20 mol% Ca, suggesting solid solution is limited up to 15 mol% of Ca under the investigated temperature. It also suggests that, the 2θ values of the doped ceria shift slightly towards higher angles when Gd and Ca content increase from 0 to 15%. The presented results in Fig. 2 follow Vegard's rule which indicate that gadolinium and calcium are well entered into the crystal lattice of ceria.

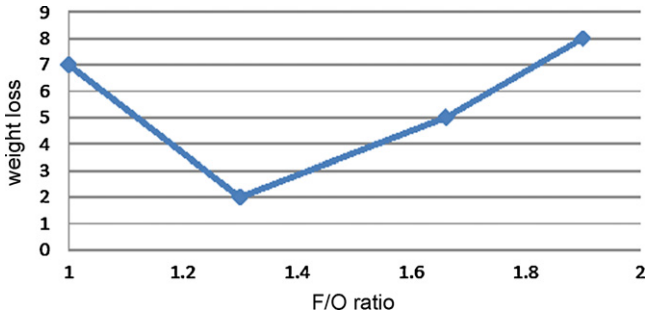

Fig. 4. Fall in weight of sample's powders after calcination.

3.1.3. The fuel to oxidant ratio

Fig. 3 shows XRD patterns of three samples of synthesized powders through combustion of gel containing different fuel to oxidant ratios. As can be seen, much sharper peaks are observed for deficient fuel ratio (F/O = 1.3). It is probably due to thermal decomposition of some nitrates at 250 °C that causes to decrease the amount of oxidant at the moment of combustion. Thus, the most energy is obtained through combustion of gel containing deficient fuel ratio.

Fig. 4 shows the weight loss of synthesized powder after calcination. This loss is related to remove of the amount of unreacted organic compounds. It can be observed that for deficient fuel ratio, the minimum of organic compounds are released. This suggests that, for deficient fuel ratio, the reaction is more complete.

3.1.4. Calcination temperature

Fig. 5 shows XRD pattern of calcined powder at 450 °C and clearly reveals that, this temperature has not been able to form a crystalline phase completely. Consequently, three various phases (CeO_2 'Gd_2O_3' $CaCO_3$) can be observed in this pattern. But for calcined powder at 850 °C, as we observed in Fig. 1, a single phase of doped ceria was formed in this temperature.

To reach an optimum calcination temperature, the relationship between lattice parameter and temperature was studied. Fig. 6

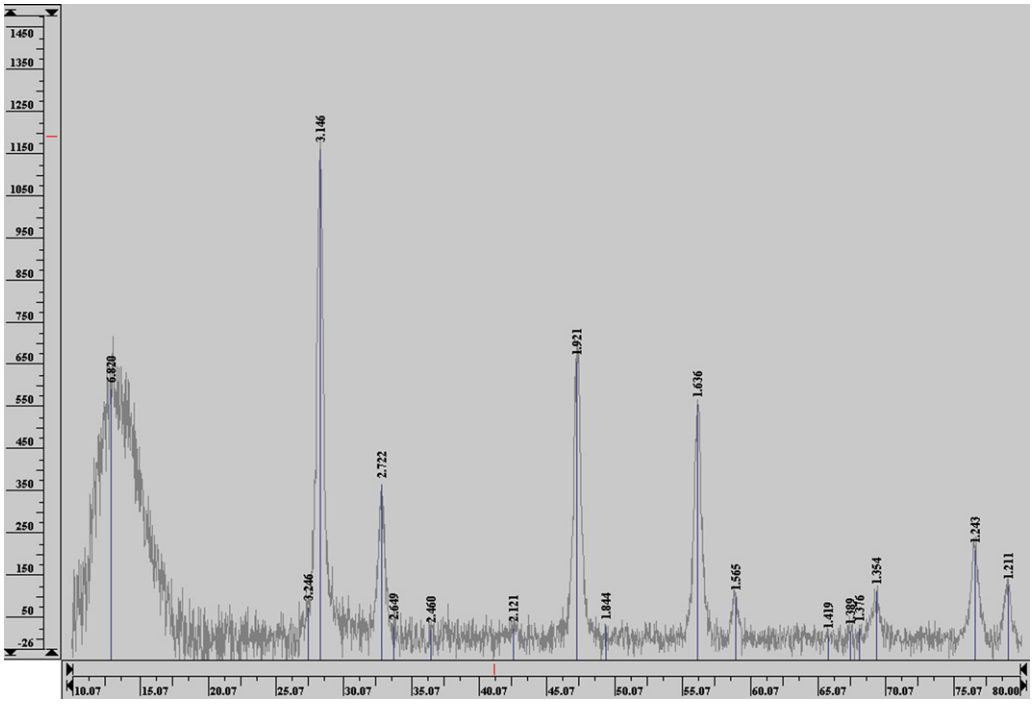

Fig. 5. XRD patterns of synthesized powder and calcined at 450 °C.

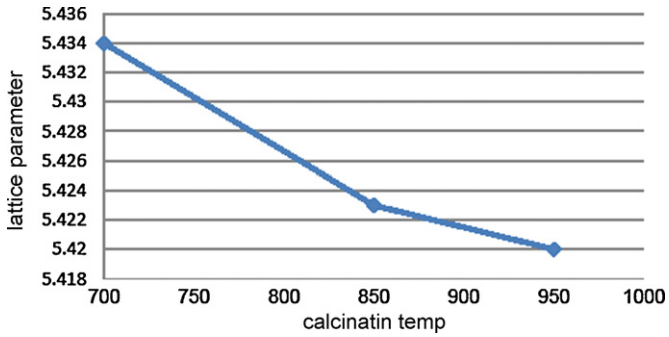

Fig. 6. Changes of lattice parameter versus calcination temperature.

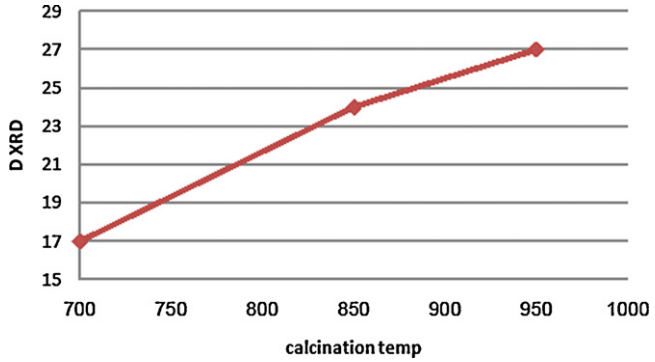

Fig. 7. Crystallite size of calcined powder in different temperatures.

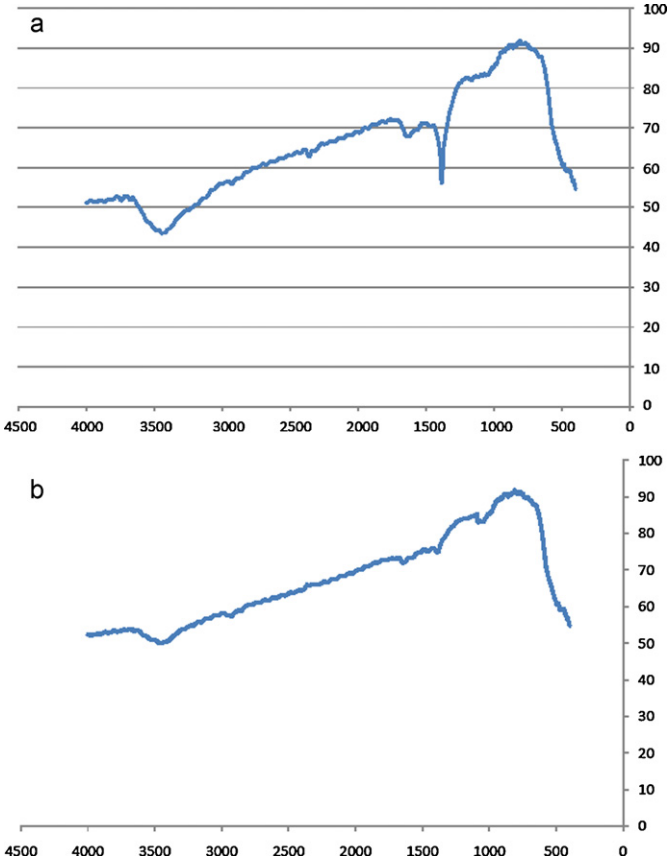

Fig. 8. FT-IR spectrum of (a) as-synthesized powder, (b) calcined powder at 850 °C.

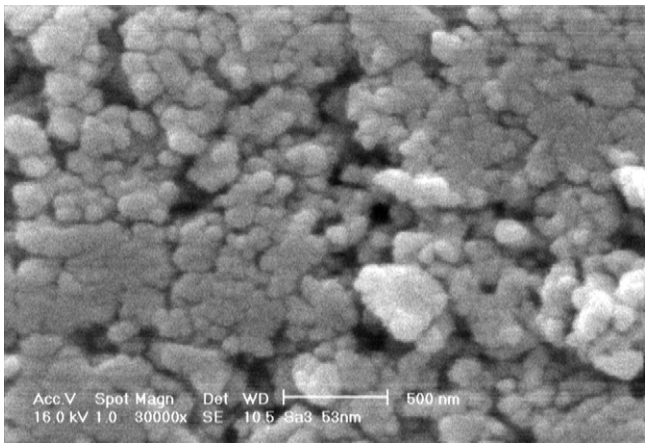

Fig. 9. SEM micrograph of calcined powder at 850 °C.

shows the changes of lattice parameter versus calcination temperature, and Fig. 7 indicates the crystallite sizes of calcined powders as a function of calcination temperature.

It can be seen that, the lattice parameters is decreased with increasing calcination temperature. Probably, this is due to formation of Ca-enriched precipitations. Crystallite size is also increased with increasing calcination temperature that accompanied with broader peaks in XRD patterns and growing particles in SEM results. Based on these results, the most appropriate calcination temperature to achieve the well-improved powder is 850 °C.

3.2. FT-IR studies

Fig. 8a shows the FT-IR spectrum of synthesized powder. Peaks which are related to nitrate is observed in 1400 cm^{-1} and that of CO grope is in 1600 cm^{-1}. These observations suggest that some of the organic matters have been resided in the sample. Fig. 8b shows FT-IR spectrum of calcined powder at 850 °C. As can be seen, there are not any residual organic matters in the sample. Also Peak attributed to Ce–O is seen at around 650 cm^{-1}.

3.3. Morphological studies

Fig. 9 shows the SEM micrograph of calcined powder's sample which indicates particles with spherical shape which are almost 40–60 nm in diameter. These observations are in accordance with XRD results.

4. Conclusion

In this work, we successfully synthesized a series of Gd and Ca co-doped cerium oxide by a combustion technique for the first time, under different conditions. The influence of the fuel to oxidant ratio on the properties of the resulted powder is discussed.

We also investigated the role of different effects on combustion process and on resulted powder. We found out, for example, the optimum calcination temperature to form a single crystalline phase is 85 °C. Some other parameters are also discussed in this paper.

References

[1] J. Van herle, T. Kawada, N. Sakai, H. Yokokawa, M. Dokiya, Solid State Ionics 86–88 (1996) 1255–1258.
[2] B.C.H. Steele, Solid State Ionics 129 (2000) 95–110.
[3] I. Hideaki, T. Hiroaki, Solid State Ionics 83 (1996) 1–16.
[4] H. Inaba, H. Tagawa, Solid State Ionics 83 (1996) 1–16.
[5] J. Herle, D. Seneviratne, A.J. McEvoy, J. Eur. Ceram. Soc. 19 (1999) 837–841.
[6] F.Y. Wang, S. Chen, S. Cheng, Electrochem. Commun. 6 (2004) 743–746.
[7] F.Y. Wang, S. Chen, Q. Wang, S.X. Yu, S. Cheng, Catal. Today 97 (2004) 189–194.

[8] M.D. Hurley, D.K. Hohnke, J. Phys. Chem. Solids 41 (1980) 1349–1353.
[9] H. Yahiro, T. Ohuchi, K. Eguchi, H. Arai, J. Mater. Sci. 23 (1988) 1036–1041.
[10] W. Huang, P. Shuk, M. Greenblatt, Solid State Ionics 113–115 (1998) 305–310.
[11] C. Peng, Y.N. Liu, Y.X. Zheng, Mater. Chem. Phys. 82 (2003) 509–514.
[12] J.A. Rodriguez, X. Wang, J.C. Hanson, G. Liu, A.I. Juez, M.F. Garcia, J. Chem. Phys. 119 (2003) 5659–5669.
[13] M. Yamashita, K. Kameyama, S. Yabe, S. Yoshida, Y. Fujishiro, T. Kawai, T. Sato, J. Mater. Sci. 37 (2002) 683–687.
[14] T. Sato, T. Katakura, S. Yin, T. Fujimoto, S. Yabe, Solid State Ionics 172 (2004) 377–382.
[15] D.A. Fumo, M.R. Morelli, A.M. Segadaes, Mater. Res. Bull. 31 (1996) 1243–1255.
[16] D.A. Fumo, J.R. Jurado, A.M. Segadaes, J.R. Frade, Mater. Res. Bull. 32 (1997) 1459–1470.
[17] J.R. Jain, K.C. Adiga, V.R. Pai Verneker, Combust. Flame 40 (1981) 71–79.
[18] S. Banerjee, P.S. Devi, Solid State Ionics 179 (2008) 661–669.
[19] M.G. Chourashiya, J.Y. Patil, S.H. Pawar, L.D. Jadhav, Mater. Chem. Phys. 109 (2008) 39–44.
[20] T. Zhang, L. Kong, Z. Zeng, H. Huang, P. Hing, Z.T. Xia, J.A. Kilner, J. Solid State Electrochem. 7 (2002) 348–354.
[21] E. Chinarro, J.R. Jurado, M.T. Colomer, J. Eur. Ceram. Soc. 27 (2007) 3619–3623.
[22] L.D. Jadhav, M.G. Chourashiya, K.M. Subhedar, A.K. Tyagi, J.Y. Patil, J. Alloys Compd. 470 (2009) 383–386.
[23] B.D. Cullity, Elements of X-ray Diffraction, Addison-Wesley, Reading, MA, 1956.
[24] P. Dattaa, P. Majewski, F. Aldinger, Mater. Charact. 60 (2009) 138–143.
[25] M. Yan, T. Mori, F. Ye, D.R. Ou, J. Zou, J. Drennan, J. Eur. Ceram. Soc. 28 (2008) 2709–2716.
[26] X. Hongmei, Y. Hongge, C. Zhenhua, Solid State Sci. 10 (2008) 1179–1184.